Toxicology in Vitro 68 (2020) 104963

Contents lists available at ScienceDirect

Toxicology in Vitro

journal homepage: www.elsevier.com/locate/toxinvit

Effects of pulse-modulated radiofrequency magnetic field (RF-EMF) exposure on apoptosis, autophagy, oxidative stress and electron chain transport function in human neuroblastoma and murine microglial cells

Jana Zielinski[a], Angélique D. Ducray[a], Anja M. Moeller[a], Manuel Murbach[b], Niels Kuster[b], Meike Mevissen[a,*]

[a] Veterinary Pharmacology and Toxicology, Vetsuisse Faculty, University of Bern, Laenggassstrasse 124, 3012 Bern, Switzerland
[b] Department of Information Technology and Electrical Engineering, Swiss Federal Institute of Technology (ETH), Rämistrasse 101, Zurich 8092, Switzerland

ARTICLE INFO

Keywords:
Radiofrequency electromagnetic fields
Neurodegeneration
Apoptosis
Oxidative stress
Autophagy
Brain cells

ABSTRACT

The use of body-worn wireless devices with different communication protocols and rapidly changing exposure scenarios is still multiplying and the need to identify possible health effects of radiofrequency electromagnetic field (RF-EMF) exposure with extremely low-frequency (ELF) modulation envelops. In this study, effects of ELF-modulated 935 MHz RF-EMF on apoptosis, autophagy, oxidative stress and electron exchange in N9 microglial and SH-SY5Y neuroblastoma cells were investigated.

Cells were exposed at 4 W/kg or sham-exposed for 2 and 24 h. RF-EMF exposure of both cell types did not alter apoptosis, the number of living cells nor the apoptosis-inducing factor (AIF), irrespective of the exposure duration. RF-EMF exposure for 24, but not for 2 h, increased protein levels of the autophagy marker ATG5, whereas LC3B-I and II and pERK were not altered in both cell types and exposure times investigated. A transient increase in glutathione (GSH), but not hydrogen peroxide and cytochrome *c* oxidase was found only in SH-SY5Y cells, indicating that short-time RF-EMF at SAR levels accepted by today's safety guidelines might cause autophagy and oxidative stress with the effect being dependent on cell type and exposure duration.

Further studies are needed to evaluate possible underlying mechanisms involved in pulse-modulated RF-EMF exposure.

1. Introduction

In recent years, exposure to radiofrequency electromagnetic fields (RF-EMF) has increased owing to new communication technologies, especially mobile phones (uplink) and base stations (downlink) (Neubauer et al., 2007). At the same time, increased exposure to RF-EMF has led to society's growing concern about the possible effects it may have on human health (Roosli et al., 2010). In 2012, the International Agency for Research on Cancer (IARC) classified non-ionizing radiofrequency radiation as possibly carcinogenic (Baan et al., 2011; IARC Working Group on the Evaluation of Carcinogenic Risks to Humans, 2013).

Besides cancer, neurodegenerative disorders, including Alzheimer's and Parkinson's disease, were demonstrated to be accompanied by neuroinflammation (Mhatre et al., 2004), and oxidative stress has been related to the etiology of neurodegenerative diseases (Dias et al., 2013; Lugrin et al., 2014; Cacabelos, 2017; Islam, 2017). Neurodegenerative diseases have been linked to an imbalance between production of

Abbreviations: AIF, Apoptosis inducing factor; Bax, Bcl-2-associated X protein; Bcl-2, B-cell lymphoma 2; DIV, Day in vitro; DNA, Deoxyribonucleic acid; DMEM, Dulbecco's Modified Eagle Medium; ELF, Extremely low-frequency; ERK (ERK1/2), pERK1/2, Extracellular signal regulated kinases, phosphorylated extracellular signal regulated kinases; FACS, Fluorescence-activated cell sorting; FBS, Fetal bovine serum; GSH, Glutathione; GSM, Global system for mobile communications; Hb-EGF, Heparin-binding epidermal growth factor; HRP, Horseradish peroxidase; IARC, International Agency for Research on Cancer; LC3B, Long chain 3B; MAPK, Mitogen-activated protein kinases; MMPs, Matrix metalloproteinases; NADPH, Nicotinamide adenine dinucleotide phosphate; NC, Negative control; OD, Optical density; PC, Positive control; RF-EMF, Radiofrequency electromagnetic fields; ROS, Reactive oxygen species; SAR, Specific absorption rate; SOD, Superoxide dismutase; TPA, 12-O-tetradecanoylphorbol 13-acetate; TRPV1, Transient receptor potential vanilloid 1

* Corresponding author at: Division Veterinary Pharmacology & Toxicology, Department of Clinical Research and Veterinary Public Health, Vetsuisse Faculty, University of Bern, Laenggassstrasse 124, 3012 Bern, Switzerland.

E-mail addresses: jana.zielinski@gmail.com (J. Zielinski), angelique.ducray@vetsuisse.unibe.ch (A.D. Ducray), anjamamoe@gmail.com (A.M. Moeller), manuel@murbach.eu (M. Murbach), kuster@itis.swiss (N. Kuster), meike.mevissen@vetsuisse.unibe.ch (M. Mevissen).

https://doi.org/10.1016/j.tiv.2020.104963
Received 10 June 2020; Received in revised form 13 July 2020; Accepted 6 August 2020
Available online 08 August 2020
0887-2333/ © 2020 Elsevier Ltd. All rights reserved.

reactive oxygen species (ROS) and antioxidant defenses (Radi et al., 2014).

There is evidence from several *in vivo* and *in vitro* studies that RF-EMF lead to an increase in oxidative stress (Friedman et al., 2007; Xu et al., 2010; Consales et al., 2012; Wang and Zhang, 2017). Impaired neurite outgrowth on neuronal cells has been demonstrated in embryonic neural stem cells exposed to RF-EMF (Chen et al., 2014). Evidence from *in vitro* studies demonstrated ROS generation in SH-SY5Y cells exposed to 1800 MHz even at a low specific absorption rate (SAR) of 0.21 W/kg (Stefi et al., 2019) and at 1–6 W/kg (Marjanovic Cermak et al., 2018), and pro-inflammatory responses were found in in microglial cell and astrocytes (Lu et al., 2014). In contrast, RF-EMF exposure alone or in combination with hydrogen peroxide (H_2O_2) did not alter intracellular ROS levels in three neuronal cell lines (Kang et al., 2014) exposed to 838 and 1950 MHz at 2 W/kg and 872 MHz at 5 W/kg (Luukkonen et al., 2009).

In an Alzheimer model, male rats showed higher oxidative stress levels in the hippocampus after RF-EMF exposure (1.5–6 W/kg) with the effect being dose-dependent (Bouji et al., 2020). Similarly, increased oxidative stress was found in the hippocampus of male Wistar rats after RF-EMF exposure (1966.1 MHz, 4.0 mW/cm^2) for 2 h a day for 16 weeks (Singh et al., 2020). RF-EMF exposure at 1.13 W/kg for 60 days increased oxidative stress and apoptosis in rats, leading to neuronal damage but not DNA damage (Motawi et al., 2014). Even at low SAR levels (0.58–0.66 mW/kg), RF-EMF exposure for 60 days resulted in an increase in oxidative stress markers and a reduction in glutathione (GSH) and superoxide dismutase (SOD), inflammation and DNA damage in male Fischer 344 rats (Megha et al., 2015). Besides increased ROS levels, significant reductions of radical scavengers were found in brain samples of Sprague-Dawley rats exposed to 2.45 GHz for 4 h a day for 45 days total, resulting in impaired learning and memory and expression of anxiety behaviour (Varghese et al., 2018). On the other hand, long-term RF-EMF exposure (1950 MHz, 5 W/kg) in C57BL/6 mice for 8 months did not induce oxidative stress and DNA damage, and no changes were found for apoptosis, astrocyte or microglia neuroinflammation markers in aging brains (Jeong et al., 2018).

Neuronal differentiation was decreased in neural stem cells exposed to 900 MHz RF-EMF at 2.29 W/kg, but viability and apoptosis of neuronal stem cells did not change (Eghlidospour et al., 2017). In SH-SY5Y neuroblastoma cells, menadione-induced caspase 3 activity was not altered in RF-EMF-exposed cells (872 MHz, 5 W/kg) compared to sham-exposure, whereas significantly higher caspase 3 levels were found in fibroblasts (Hoyto et al., 2008). Similar findings were obtained in primary neurons obtained from cortices of embryonic Wistar rats. RF-EMF exposure at 900 MHz (0.25 W/kg) for 24 h did not affect apoptosis (Joubert et al., 2007). In contrast, gene expression of apoptosis markers were affected after Global System for Mobile Communications (GSM) RF-EMF radiation in SH-SY5Y cells (Buttiglione et al., 2007), mouse embryonic stem cells (Nikolova et al., 2005), primary neurons and astrocytes (Zhao et al., 2007).

Dysfunctional autophagy, an intracellular machinery for degrading damaged and aggregated proteins and organelles has been reported to be involved in the pathology of neurodegenerative disorders (Menzies et al., 2015; Guo et al., 2018; Kumar et al., 2018; Chu, 2019). Recent data showed increased levels of genes related to autophagy and autophagosomes in the hippocampus but not in the brain stem in C57BL/6 mice after RF-EMF exposure at 835 MHz (4 W/kg) for 12 weeks (Kim et al., 2018). Extracellular signal regulated kinase (ERK), localized at autophagosomes, was demonstrated to regulate autophagy through interactions of its substrate binding domain with autophagy-related (ATG) proteins (Martinez-Lopez et al., 2013). Interestingly, the mitogen-activated protein kinase (MAPK) ERK was found to be rapidly activated after RF-EMF exposure due to a cascade of cellular events triggered by ROS (Friedman et al., 2007). In contrast, MAPK phosphorylation in astrocytes was not altered after RF-EMF exposure to 1763 MHz (2 and 20 W/kg) for 30 and 60 min (Lee et al., 2006).

In this study, we investigated the effect of RF-EMF exposure at 4 W/kg (SAR) on oxidative stress, apoptosis, and autophagy and electron transport chain function in SH-SY5Y and microglial cells (N9).

2. Material & methods

2.1. Cell culture

The human neuroblastoma cell line SH-SY5Y (ATCC, USA) was cultivated in Dulbecco's Modified Eagle Medium (DMEM) GlutaMax (Gibco, Thermo Fisher, USA) with 10% Fetal bovine serum (FBS) and penicillin (100 units/mL) – streptomycin (10 µg/mL) as well as 2 mM L-Glutamine (Gibco, Thermo Fisher, USA) and 1 mM sodium pyruvate (Gibco, Thermo Fisher, USA). Cells were incubated at 37 °C under 5% CO_2.

Murine microglial cells (N9, Department of Clinical Research, University of Bern, Switzerland) were cultured in DMEM (Gibco, Thermo Fisher Scientific, USA) supplemented with 10% FBS (Gibco, Thermo Fisher Scientific, USA) and penicillin (100 units/mL) – streptomycin (10 µg/mL) (Gibco, Thermo Fisher Scientific, USA) at 37 °C under 5% CO_2.

2.2. RF-EMF exposure

The RF-EMF exposure had been selected to meet all criteria of Kuster and Schonborn (2000) with maximum induced fields below thermal threshold, large extremely low-frequency (ELF) modulation envelop with intermittent exposure while still synthesizing the exposure of a GSM wireless signal. The SH-SY5Y and N9 cells were exposed in the sXc900 exposure system (IT'IS Foundation, Zurich, Switzerland) that was fully characterized regarding electromagnetic and thermal dosimetry (Schuderer et al., 2004a) and validated prior to the experiment. The exposure signal consisted of an intermittent '"talk-mode"' GSM modulation envelope (935 MHz carrier frequency, 216.7 Hz pulse-modulated rate, where each 26th GSM frame is blanked (adding an 8 Hz modulation), ON/OFF cycles of 120/120 s. Cells were exposed at an average SAR of 4 W/kg ± 0.16 SD with a non-uniformity of the SAR distribution of 25% (Schuderer et al., 2004b) during the on-cycle, under the culture conditions described above (37 °C ± 0.1 °C, > 80% humidity, 5% CO2). The maximum thermal load of the cells in the monolayer was < 0.1 °C compared to sham (Schuderer et al., 2004b). All experiments were performed in a double-blinded fashion with two waveguide chambers for RF-EMF and sham exposure, respectively and eight cell culture dishes (35 mm) (Thermo Fisher Scientific, Massachusetts, USA) per chamber, containing 4 ml medium per dish. Cells were plated on day *in vitro* (DIV) 0, RF-EMF or sham exposure started 24 h after plating, and measurements were performed at the end of the exposure.

2.3. Apoptosis

SH-SY5Y and N9 cells were seeded to obtain 3.10^6 and $1.2.10^6$ cells per 35 mm dish in 4 mL DMEM GlutaMax or DMEM, respectively after RF-EMF or sham exposure. Following RF-EMF at SAR of 4 W/kg or sham exposure, cells were trypsinized and washed once with 1× phosphate buffered saline (PBS, Gibco, Thermo Fisher, USA). At both time points (2 and 24 h), four sample groups were investigated, namely RF-EMF- and sham-exposed cells as well as cells treated with 1 µM staurosporine (Sigma, Switzerland), functioning as a positive control (PC) in combination with RF-EMF and sham exposure. Cells were counted and 1.10^5 cells of all sample groups were investigated with the Dead Cell Apoptosis Kit (Molecular Probes, Thermo Fisher Scientific, USA). The cell staining was processed in accordance to the manufacturer's data sheet. Briefly, Alexa Fluor® 488 Annexin V (FITC, green) was detected by the laser Coherent® to identify apoptotic cells, whereas propidium iodide (PI, red) was detected by the laser Sapphire™ and

served as the live/dead discriminator. The gating was set for living cells FITC neg/PI neg, for early apoptotic cells FITC pos/PI neg and for dead and late apoptotic cells FITC pos/PI pos. All samples were incubated with the provided buffer system for 15 min at room temperature (RT) and subsequently kept on ice until further investigated using a BD LSR II flow cytometer (BD Biosciences, Belgium) and analysed by FlowJo 7.6 software (FlowJo, LLC, USA).

2.4. Apoptosis and autophagy

2.4.1. Apoptosis inducing factor (AIF)

SH-SY5Y and N9 cells were seeded to obtain 3.10^6 and $1.2.10^6$ cells per 35 mm dish in 4 mL DMEM GlutaMax or DMEM, respectively after RF-EMF or sham exposure. A positive control was conducted by incubating N9 cells with 2.5 μM staurosporine and SH-SY5Y cells with 0.1 μM staurosporine for 6 h at 37 °C with 5% CO_2. Following RF-EMF at SAR of 4 W/kg or sham exposure or staurosporine exposure, cells were washed once with 1× PBS. Protein was extracted by scraping off the cells of all eight dishes per irradiation chamber or chemical exposure in 100 μL resuspension buffer (containing 2 mM HEPES and 0.2 mM EGTA supplemented with 1× HALT protease inhibitor and 1× phosphatase inhibitor cocktails). Subsequently, the samples were sonicated once with 10% power for 10 s and centrifuged at 200×*g* for 7 min. The supernatant of each sample was transferred into a new vial and the pellet was washed with 100 μL resuspension buffer. Afterwards, the samples were sonicated again with 10% power for 10 s, incubated on ice for 30 min, rigorously vortexed for 15 s and centrifuged at 800×*g* for 15 min. The resulting pellets of centrifugation one and two were pooled and the produced supernatant was centrifuged at 2′500×*g* for 10 min. The pellets were pooled and sonicated twice with 10% power for 10 s. The resulting supernatant was centrifuged at 13′200×*g* for 20 min. The supernatant fraction, containing the cellular proteins, was sonicated twice with 10% power for 10 s. The protein amount was obtained with Pierce™ 660 nm Protein Assay Reagent.

Nuclei and cytosolic fractions were processed for Western Blotting. After the successful transfer, the nitrocellulose membrane was blocked for 2 h at RT in 5% milk powder diluted in 1× PBS (Thermo Fisher Scientific, Switzerland), containing 0.2% Tween (Sigma, Switzerland). Subsequently, the primary antibody AIF (Cell Signaling Technology, USA), was diluted in the blocking solution 1:500 and incubated overnight on a rocker at 4 °C. The membrane was rinsed twice and washed three times for 5 min in 1 x PBS, 0.2% Tween before anti-β-actin (Sigma, Switzerland) was diluted 1:4′000 in the blocking solution and incubated for another 2 h at RT. Secondary antibodies, donkey-anti-rabbit and goat-anti-mouse horseradish peroxidase (HRP) (Jackson Laboratories, USA), were diluted 1:10′000 in the blocking solution and applied at RT for 2 h.

Detection of the respective protein was achieved by incubation with Immobilon Western Chemiluminescent HRP Substrate (Millipore Merck, Switzerland) and analysed by the LAS-3000 Imaging System (Fuji, Germany).

Quantification of the protein amount was performed using Image J software (National Institutes of Health, Washington, USA) and normalizing the optical density (OD) of the investigated protein band with the OD of the β-actin band of the same sample on the same membrane.

2.4.2. Autophagy-related protein 5 (ATG5), light chain 3B (LC3B) and extracellular signal–regulated kinases (ERK)

SH-SY5Y and N9 cells were seeded to obtain 3.10^6 and $1.2.10^6$ cells per 35 mm dish in 4 mL DMEM GlutaMax or DMEM, respectively after RF-EMF or sham exposure. Following RF-EMF at SAR of 4 W/kg or sham exposure, cells were washed once with 1× PBS. Protein was extracted by scraping off the cells of all eight dishes per chamber in 100 μL lysis buffer (Sigma, Switzerland) supplemented with 1× HALT protease inhibitor and 1× phosphatase inhibitor cocktails. Subsequently, the samples were sonicated twice (10% power) for 4 s and afterwards centrifuged for 10 min at 13′200×*g*. The supernatant was transferred into a new test tube and 10 μL were used for protein measurements with Pierce™ 660 nm Protein Assay Reagent (Thermo Fisher Scientific, Switzerland).

Table 1
Antibodies.

	Antibody	Host	Company	Dilution
Primary	p53	Mouse	Santa Cruz	1:500
	ATG5	Mouse	R&D systems	1:1000
	Bcl2	Mouse	Abcam	1:1000
	Bax	Rabbit	Cell signaling	1:1000 (SH-SY5Y) 1:2000 (N9)
	LC3B	Rabbit	Cell signaling	1:1000
	ERK 1/2	Mouse	Cell signaling	1:2000
	β-actin	Mouse	Sigma Aldrich	1:40,000
Secondary	Anti-mouse IgG HRP	Donkey	Novex	1:5000/1:100,000
	Anti-rabbit IgG HRP	Donkey	Novex	1:5000

Markers for autophagy (ATG5, LC3B, pERK) were analysed by Western blotting. The membranes, 0.45 μm Immobilion PVDF (Sigma, Switzerland) or nitrocellulose (Sigma, Switzerland) were washed in 1 x Tris buffered saline (TBS, pH 7.6, Sigma, Switzerland) with 0.5% Tween (Sigma, Switzerland) and blocked for 2 h at RT in 5% milk powder (Migros, Switzerland) in 25 mM Tris (Sigma, Switzerland), pH 7.4, 0.15 M NaCl (Sigma, Switzerland), 0.1% Tween. Subsequently, the primary antibodies, shown in Table 1, were incubated on a rocker over night at 4 °C. The monoclonal mouse antibody anti-β-actin (Sigma, Switzerland) was diluted 1:500′000 in 1 x TBS and incubated for 2 h at RT.

The secondary antibodies, donkey-anti-rabbit and goat-anti-mouse HRP (Jackson Laboratories, USA), were diluted 1:10′000 in 1 x TBS with 0.5% Tween and applied at RT for 2 h (β-actin 1 h). Detection and quantification were achieved as previously described (Zielinski et al., 2016).

2.5. Oxidative stress

2.5.1. GSH

Cellular GSH levels were measured to detect an induction of oxidative stress. The assay was based on the conversion of a luciferin derivative into luciferin in the presence of GSH. Luminescence is proportional to the amount of GSH present in the cells.

SH-SY5Y and N9 cells were seeded to obtain 3.10^6 and $1.2.10^6$ cells per 35 mm dish in 4 mL DMEM GlutaMax or DMEM, respectively, after RF-EMF or sham exposure. Following RF-EMF at SAR of 4 W/kg or sham exposure, cells were trypsinized and washed once with 1× PBS. Exposed and sham-exposed cells (50 μL) were added to a 96-well plate (density: 10′000 cells/well), 50 μL of GSH-Glo™ Glutathione Assay (Promega, Switzerland) were added, followed by an incubation of 30 min at RT. Finally, 100 μL of reconstituted luciferase detection reagent (Promega, Switzerland) were added and incubated for 15 min at RT before luminescence was measured on a microplate reader (Synergy HT, Bio-Tek, Switzerland). Menadione, at a concentration of 50 μM and 75 μM for was used as PC for N9 cells and SH-SY5Y cells, respectively.

2.5.2. Hydrogen peroxide production

SH-SY5Y and N9 cells were seeded to obtain 3.10^6 and $1.2.10^6$ cells per 35 mm dish in 4 mL DMEM GlutaMax or DMEM, respectively after RF-EMF or sham exposure. Following RF-EMF at SAR of 4 W/kg or sham exposure, cells were washed once with cold 1× PBS. Mitochondrial protein was extracted in the same way as described for AIF. Briefly, after scraping off the cells in 100 μL resuspension buffer, the samples were sonicated and processed through several centrifugation steps. After centrifugation at 13′200×*g*, the pellets were resuspended in 50 μL mitochondrial buffer, containing 5 μM $MgCl_2$ and

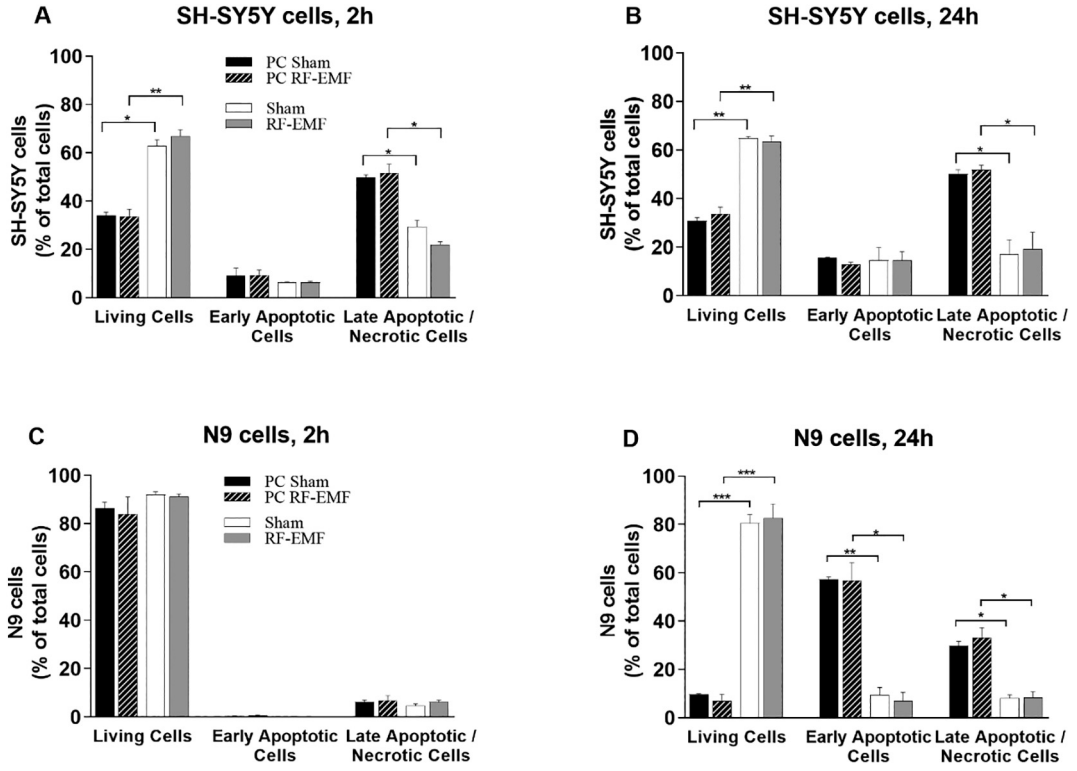


Fig. 1. Fluorescence-activated cell sorting (FACS) data analysis of RF-EMF and sham-exposed SH-SY5Y cells at 4 W/kg for 2 h (A) and 24 h (B) and of N9 cells for 2 h (C) and 24 h (D). Staurosporine-treated cells were used as positive control (PC) with sham- (PC sham, black bars) and RF-EMF- (PC RF-EMF, black-striped bars) exposed cells and non-treated sham- (sham, white bars) and RF-EMF- (RF-EMF, grey bars) exposed cells are depicted in the histograms. Cell sorting was performed to obtain living cells, early apoptotic cells and late apoptotic/necrotic cells. Error bars represent the standard error of the mean (SEM). Significant differences are labeled with asterisks (A-B:* = $p \leq 0.001$; ** = $p \leq 0.0001$_ C-D: * = $p \leq 0.01$; ** = $p \leq 0.001$; *** = $p \leq 0.0001$).

2.5 mM H_2KPO_4 (Merck, Germany) as well as protease and phosphatase inhibitor cocktails as described for the resuspension buffer. The mitochondrial fraction was incubated in an ultrasonic water bath (Sonorex Super, Brandelin, Switzerland) for 5 min and 10 µL were used for protein measurements with Pierce™ 660 nm Protein Assay Reagent. The remaining sample was used for measurements with the Amplex Assay (Thermo Fisher Scientific, Switzerland) or the cytochrome *c* oxidase activity assay (Sigma, Switzerland) for N9 cells only.

Samples for H_2O_2 measurements were processed as stated in the manufacturer's data sheet. Briefly, a standard curve ranging from 0 to 2 µM H_2O_2 was prepared. Standard samples and mitochondrial fractions, topped with 1× reaction buffer (provided by the assay) to reach set assay volume of 50 µL, were loaded onto a 96 well plate. Finally, freshly prepared working solution of 100 µM Amplex® Red reagent (*N*-acetyl-3,7- dihydroxyphenoxazine) and 0.2 U/mL HRP (both provided by the assay) was added to the wells and incubated in the dark for 30 min at RT. The samples were measured with the emission at 530 nm and excitation at 590 nm with a Synergy H1 multi-mode reader (BioTek, Switzerland). The none-H_2O_2 control was subtracted as background of each sample and the values were quantified by the help of the standard curve equation. To follow the kinetics of the continuous reaction, additional measurements were done after 60 and 90 min.

2.6. Cytochrome c oxidase activity

Cytochrome c oxidase activity was measured in mitochondrial samples using the cytochrome *c* oxidase assay (Sigma-Aldrich, Switzerland). The enzyme is reduced with DTT and then reoxidized by the cytochrome *c* oxidase. The colorimetric assay is based on the decrease in absorbance of ferrocytochrome *c* caused by its oxidation to ferricytochrome *c*.

N9 cells were seeded to obtain $1.2.10^6$ cells per 35 mm dish in 4 mL DMEM after RF-EMF or sham exposure, and the mitochondrial protein fraction was produced as described above.

Samples were processed according to the manufacturer's instructions. Briefly, 1× assay buffer (provided by the assay) was mixed with the mitochondrial fraction and adjusted to the final reaction volume with 1× enzyme dilution buffer. The reaction was started by adding ferrocytochrome *c* substrate solution (provided by the assay) to the mix and read immediately at 550 nm with a Synergy H1 multi-mode reader and the enzyme activity was calculated in units with one unit being defined to oxidize 1.0 mmol of ferrocytochrome c per minute at pH 7.0 at 25 ˚C.

2.7. Statistics

Three independent experiments were performed for each group and all parameters investigated. Data were analysed with GraphPad Prism (version 6.0, La Jolla, California, USA) using a two-way ANOVA with Tukey's multiple comparisons test, one-way ANOVA with Sidak's multiple comparison test or Kruskal Wallis with Dunn's multiple comparison test. *P* values ≤ 0.05 were considered significant.

3. Results

3.1. Apoptosis

Apoptotic cells were quantified by annexin-V (FITC) and propidium iodide (PI) co-staining. Living cells (FITC neg/PI neg), early- (FITC pos/PI neg), and late- apoptotic as well as necrotic cells (FITC pos/PI pos) were identified as the fluorophore labeled annexin binds specifically to phosphatidyl serine, which transfers from the inner to the outer leaflet in cells undergoing apoptosis, whereas PI binds to nucleic acid and is impermeable to living cells.

As expected, a significant decrease ($p \leq 0.001$) in the fraction of living cells was found in staurosporine-treated PCs compared to RF-EMF- and sham-exposed SH-SY5Y cells as shown in Fig. 1A-B. Furthermore, a significant increase ($p \leq 0.01$) in the percentage of late-apoptotic and necrotic cells was demonstrated when SH-SY5Y staurosporine-treated cells were compared to their respective controls, namely sham and RF-EMF at both exposure times (Fig. 1A-B). No significant difference was found between any of the groups for early apoptosis for both times investigated.

In N9 cells, no significant differences between staurosporine-treated cells were found for living cells, early apoptotic cells and late apoptotic cells after a 2-h exposure when sham- and RF-EMF-exposed cells were compared as illustrated in Fig. 1C. The percentage of living cells of RF-EMF-exposed N9 cells for 2 h was 80–90% were regardless of treatment with staurosporine. The percentage of early and late-apoptotic cells was 1–2% and 5–10%, respectively for all groups for a 2-h exposure. In contrast, RF-EMF- and sham-exposed N9 cells incubated with staurosporine for 24 h resulted in a significant decrease in living cells ($p \leq 0.0001$), but no effect between RF-EMF and sham exposure was found (Fig. 1D). Staurosporine treatment led to a significant increase in early apoptotic cells (~60%; $p \leq 0.001$) and late apoptotic N9 cells (~30%, $p \leq 0.01$), but no difference was found after a 24-h exposure of N9 cells when RF-EMF and sham exposure were compared (Fig. 1D).

Apoptosis inducing factor (AIF) was measured in the nuclei fraction of RF-EMF- and sham-exposed cells for 2 and 24 h. Staurosporine-treated cells were used as PCs (Fig. 2). Measurements in the cytosolic fraction showed no AIF content. As expected, a significant increase in AIF expression ($p \leq 0.001$) was observed after treatment with staurosporine in SH-SY5Y cells when compared to the negative control

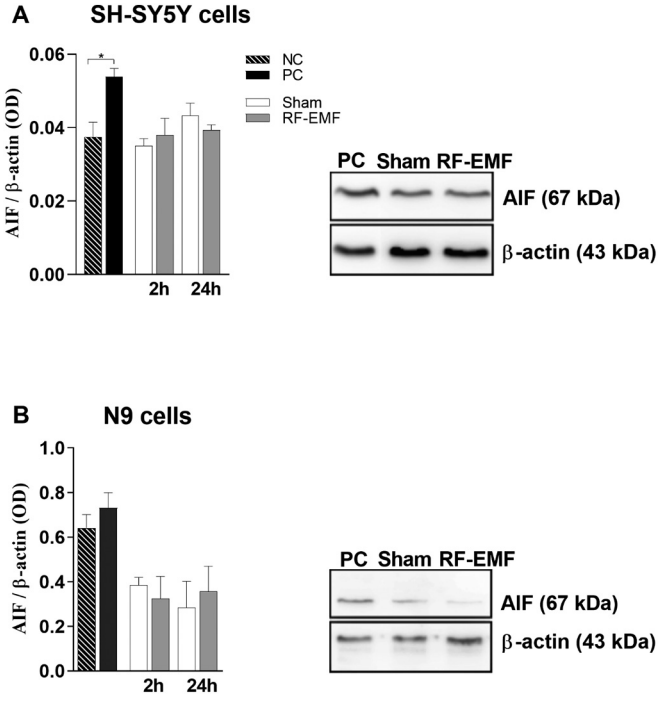


Fig. 2. Protein expression of apoptosis inducing factor (AIF, 67 kDa) of SH-SY5Y cells (A) and N9 cells (B) that were RF-EMF (RF-EMF, grey bars) and sham-exposed at 4 W/kg for 2 and 24 h (sham, white bars). Representative Western blot images after 24 h of exposure are given on the right. Histograms depict the mean optical density (OD) of the signal normalized to the β-actin signal OD of the same sample. Non-treated control cells were used as negative control (NC, black-striped bar), and staurosporine-treated cells were used as positive control (PC, black bar) and both were sham-exposed. Error bars represent the standard error of the mean (SEM). Significant differences are labeled with asterisks (* = $p \leq 0.05$).

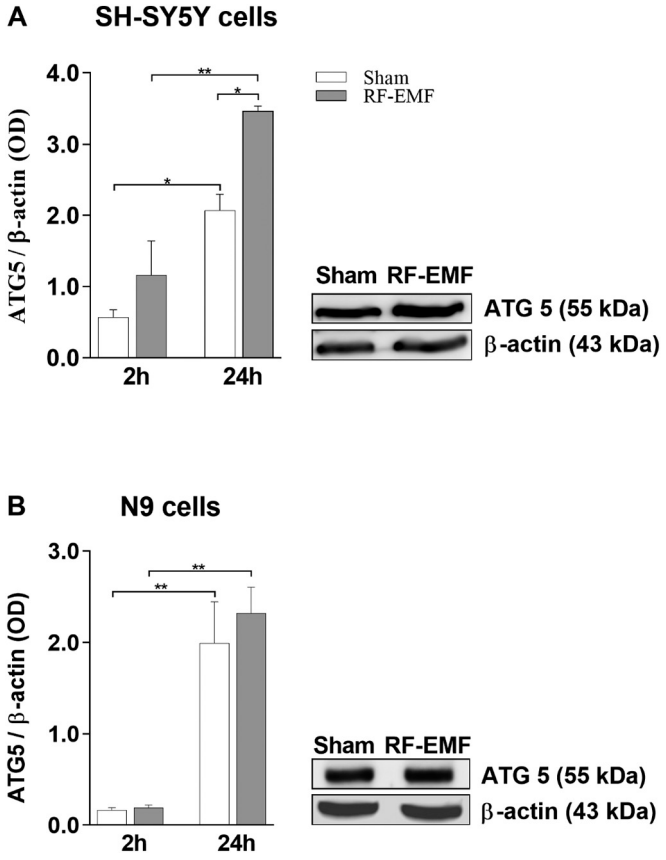


Fig. 3. Representative Western blot images of the autophagy protein 5 (ATG5) after 24-h RF-EMF and sham exposure are illustrated for SH-SY5Y (A) and N9 (B) cells. Histograms depict the mean optical density (OD) of the ATG5 signal, normalized to the β-actin signal of the same sample under sham-exposure (white bars) and RF-EMF- (black bars) exposure at 4 W/kg for 2 and 24 h. Error bars represent the standard error of the mean (SEM). Significant differences are labeled with asterisks (* = $p \leq 0.05$; ** = $p \leq 0.01$).

(Fig. 2A) but not in N9 cells (Fig. 2B). No difference in AIF expression was observed between sham- and RF-EMF-exposed samples for both cell types at both exposure times (Fig. 2A-B).

Investigations on the protein amount of the apoptosis markers B-cell lymphoma 2 (Bcl-2), Bcl-2-associated X protein (Bax) and the tumor-suppressor gene p53 revealed no differences between RF-EMF- and sham-exposed cells regardless of cell type and exposure (data not shown).

3.2. Autophagy

Autophagy markers, including ATG5 and LC3B-I and II and pERK were analysed in RF-EMF and sham-exposed SH-SY5Y and microglial cells. In SH-SY5Y cells, an increase in ATG5 by trend was found in RF-EMF-exposed cells after 2 h when compared to sham-exposed cells as illustrated in Fig. 3A. However, the difference was not statistically significant. No difference in ATG5 protein levels was found in RF-EMF-exposed N9 cells compared to the respective sham control at any time investigated (Fig. 3B). ATG5 protein levels in SH-SY5Y cells were significantly increased ($p \leq 0.05$) after RF-EMF exposure for 24 h compared to the respective sham control. Interestingly, ATG5 protein levels were significantly higher after 24 h of exposure, regardless of exposure and cell type (SH-SY5Y: sham $p \leq 0.05$; RF-EMF $p \leq 0.01$; N9: sham $p \leq 0.01$; RF-EMF $p \leq 0.01$) compared to 2 h (Fig. 3A and B).

A slight increase in LC3B-I was found in SH-SY5Y RF-EMF-exposed cells after 2 h of RF-EMF exposure when compared to sham-exposed cells, but this trend was not statistically significant, and no difference

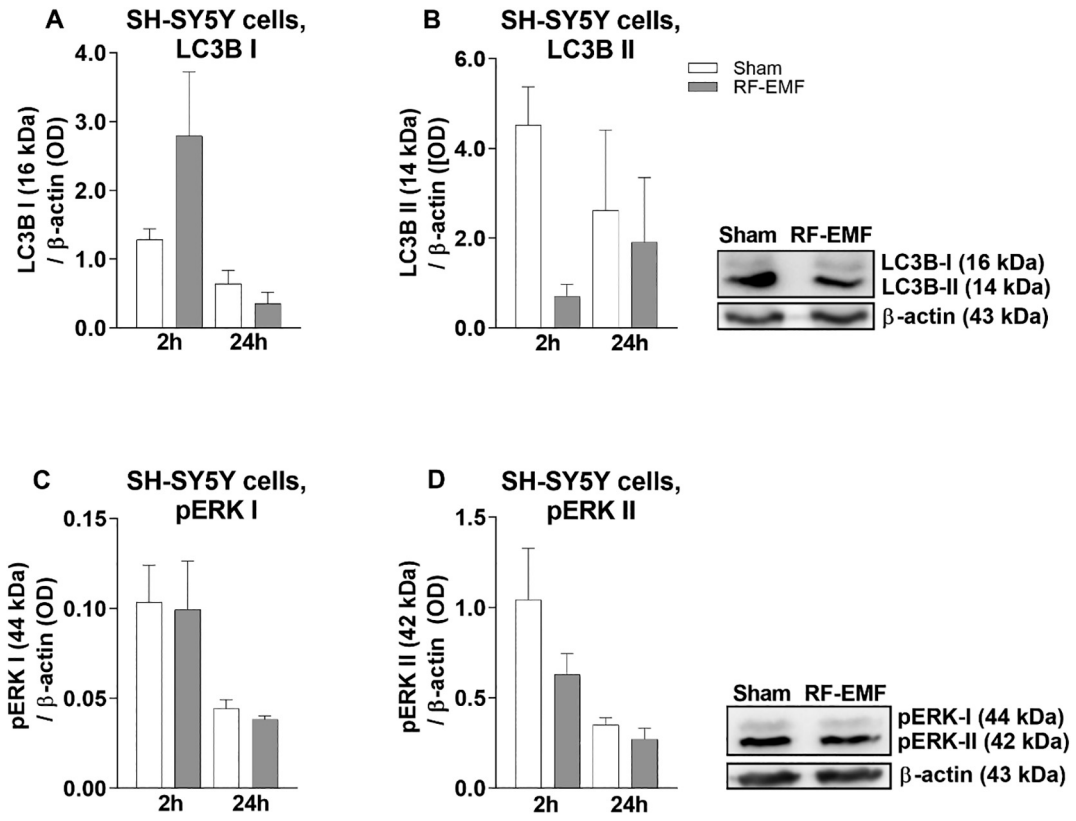


Fig. 4. Protein expression of (A) Long-Chain 3B-1 (LC3B-I, 16 kDa), (B) Long-Chain 3B-II (LC3B-II, 14 kDa) and phosphorylated extracellular signal–regulated kinases (C) I (pERK I, 44 kDa) and (D) II, (pERK II, 42 kDa) in SH-SY5Y cells. Representative Western blot images are given on the right for samples of cells that were sham- and RF-EMF-exposed for 24 h. The histograms show the mean optical density (OD) of the signal normalized to the β-actin signal OD of the same sample. SH-SY5Y cells were sham- (white bars) or RF-EMF- (grey bars) exposed at 4 W/kg for 2 and 24 h. The histograms represent sham- (sham, white bars) and RF-EMF- (RF-EMF, grey bars) exposed cells.

between these two groups was found after 24 h of exposure (Fig. 4A). A strong tendency towards a downregulation of LC3B-II was found between RF-EMF-exposed and sham-exposed SH-SY5Y cells as illustrated in Fig. 4B. However, the effect was not significant. No difference was observed after 24 h of exposure between RF-EMF- and sham-exposed cells. Protein levels of pERK I and II did not differ between sham- and RF-EMF-exposed SH-SY5Y cells, regardless of the exposure time as shown in Fig. 4C and D.

3.3. Oxidative stress

Oxidative stress was investigated by measurements of GSH and H_2O_2 levels in sham- and RF-EMF-exposed cells at 4 W/kg in both cell types.

Menadione-treatment for 6 and 24 h resulted in a significant decrease in GSH levels in SH-SY5Y (Fig. 5A) and microglial cells (Fig. 5B) when compared to the respective RF-EMF- and sham-exposed cells without menadione. A significant reduction of GSH levels was found after 6 h ($p \leq 0.05$) when RF-EMF-exposed SH-SY5Y cells were compared to sham-exposed cells (Fig. 5A). This effect was not apparent anymore after 24 h of exposure as shown in Fig. 5A. In contrast, in N9 cells, RF-EMF exposure did not change GSH levels when compared to sham-exposed cells at both exposure times (Fig. 5B).

Hydrogen peroxide levels were measured in SH-SY5Y (Fig. 6A) and N9 cells (Fig. 6B). No significant differences were found after 2 h of sham-exposure in both cell types. A significant increase in H_2O_2 levels was found after 24 h, but no significant differences were obtained between RF-EMF- and sham-exposed cells after exposure for 2 and 24 h (Fig. 6). Interestingly, H_2O_2 levels were higher in SH-SY5Y cells than in N9 cells, but undifferentiated and differentiated SH-SY5Y cells have been reported to have distinct responses to cellular stressors with differentiated cells being more stress-resistant (Schneider et al., 2011).

3.4. Cytochrome c oxidase activity

Cytochrome c oxidase was measured in the mitochondrial fraction of N9 cells. A significant decrease in cytochrome c levels was found after 2 h, but no difference was obtained after 24 h, in RF-EMF-exposed cells compared to sham-exposed cells as illustrated in Fig. 7. Cytochrome c remained low at 24 h of exposure and a significant difference was found between the sham control exposed for 2 h and the RF-EMF- ($p \leq 0.05$) sham-exposed ($p \leq 0.001$) and the cells for 24 h.

4. Discussion

In this study, we investigated the effect of intermittent and ELF-modulated RF-EMF exposure for 2 and 24 h at 4 W/kg (SAR) on oxidative stress, apoptosis, and autophagy and electron transport chain function in SH-SY5Y and microglial (N9) cells.

RF-EMF exposure did not alter proportions of early and late apoptosis and living cells when compared to sham exposure in both microglial and neuroblastoma cells. As expected, staurosporine induced apoptosis. Corroborating these data, the apoptosis markers AIF, Bcl-2 and Bax were similar in RF-EMF and sham-exposed cells, indicating that RF-EMF does not induce apoptosis in both cell types under the conditions used in this study. Similar findings were obtained in primary neurons obtained from cortices of embryonic Wistar rats at a lower SAR level (0.25 W/kg). RF-EMF exposure at 900 MHz for 24 h did not affect apoptosis (Joubert et al., 2007). RF-EMF exposure (900 MHz RF-EMF at 2.29 W/kg) has been shown to reduce neuronal differentiation but

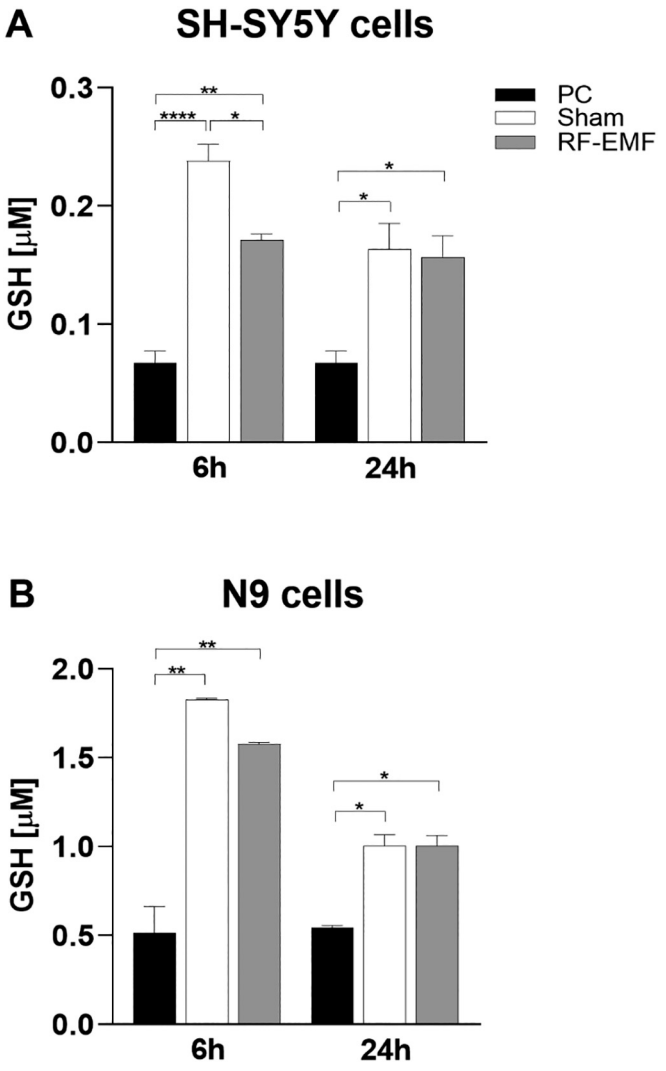


Fig. 5. SH-SY5Y cells (A) and N9 cells (B) were sham- (white bars) and RF-EMF-exposed (grey bars) at 4 W/kg for 6 and 24 h. Glutathione levels (GSH) were measured at the end of the RF-EMF- or sham exposure. Menadione [75 µM] was used as a positive control (PC, black bars). Data are shown as extrapolated GSH levels [µM] for each group. Error bars represent the standard error of the mean (SEM) (n = 3 from 3 independent experiments). Significant differences are labeled with asterisks (* = $p \leq 0.05$; ** = $p \leq 0.01$; *** = $p \leq 0.001$).

viability and apoptosis of neuronal stem cells remained unchanged (Eghlidospour et al., 2017). In SH-SY5Y neuroblastoma cells, menadione-induced caspase 3 activity was not altered in RF-EMF-exposed cells (872 MHz, 5 W/kg) compared to sham-exposure, supporting our findings. On the other hand, significant higher caspase 3 levels were found in fibroblasts (Hoyto et al., 2008), indicating the effect depending on the cell type.

In contrast to our findings, in SH-SY5Y cells gene expression of the inhibitory apoptosis markers Bcl-2 and surviving were lowered after 900 MHz-modulated RF-EMF radiation at a substantially lower SAR (0.35 W/kg) (Buttiglione et al., 2007). In mouse embryonic stem cells, RF-EMF exposure of 1.17 GHz and 1.5 W/kg transiently increased the transcript levels of genes related to apoptosis and DNA damage was seen after RF-EMF exposure for 6 but not for 24 h (Nikolova et al., 2005). Gene expression does not necessarily account for protein expression and might explain the different findings. In primary neurons, 1900 MHz RF-EMF exposure for 2 h upregulated certain apoptosis markers with neurons being more sensitive than astrocytes (Zhao et al., 2007). In contrast to our study, no dosimetry was performed and RF-

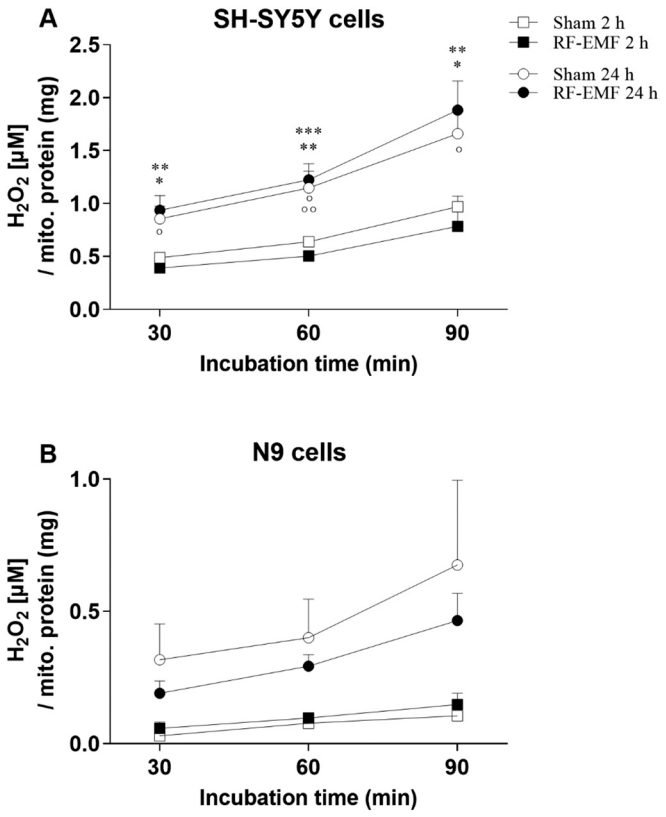


Fig. 6. Peroxide (H_2O_2)/peroxidase production was measured in SH-SY5Y cells (A) and N9 cells (B) after sham (white symbols) and RF-EMF-(black symbols) exposure at 4 W/kg for 2 h (square symbols) and 24 h (round symbols). Graphs are showing H_2O_2 concentrations in [µM] for each group normalized to the total mitochondrial (mito.) protein content in milligram (mg). Error bars represent the standard error of the mean (SEM). Significant differences regarding exposure time of either sham-irradiated cells and RF-EMF- exposed cells are labeled with circles (° = $p \leq 0.05$; °° = $p \leq 0.01$). Significant differences between RF-EMF-exposed cells exposed for 24 h to sham- or RF-EMF-exposed cells for 2 h are labeled with asterisks (* = $p \leq 0.05$; ** = $p \leq 0.01$; *** = $p \leq 0.001$).

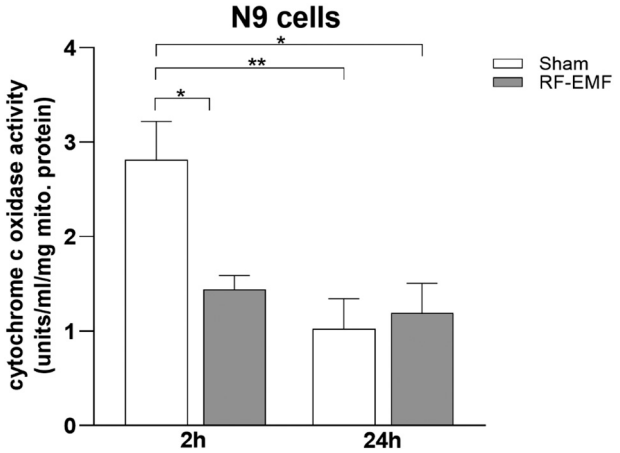


Fig. 7. Cytochrome c oxidase activity was measured in sham-exposed N9 cells-(white bars) and RF-EMF- (grey bars) exposed cells at 4 W/kg for 2 and 24 h. Data for each group were normalized to the total mitochondrial (mito.) protein content in milligram (mg) and are shown as cytochrome c oxidase activity in units/µl/mg mito. Protein. Error bars represent the standard error of the mean (SEM) (n = 6). Significant differences are labeled with asterisks (* = $p \leq 0.05$; ** = $p \leq 0.001$).

EMF exposure was done putting a cell phone in the 'on' mode or the 'stand by' mode on top of the petri dish with the cells. Ertilav et al. proposed a mechanism including the dose-dependent activation of the TRPV1 channel resulting in oxidative stress, apoptosis and increased intracellular calcium levels in hippocampal and dorsal root ganglion neurons after exposure to 900 and 1800 MHz at 0.1 W/kg whole-body average SAR (Ertilav et al., 2018). Moreover, evidence from *in vivo* findings also did not demonstrate changes in apoptosis markers, astrocyte or microglia neuroinflammation marker in aging brains of C57BL/6 mice exposed to RF-EMF exposure (1950 MHz, 5 W/kg) for 14 months (Jeong et al., 2018). In contrast, RF-EMF exposure of rats at 1.13 W/kg for 60 days increased oxidative stress and apoptosis in the brain, but did not lead to DNA damage but neuronal damage (Motawi et al., 2014).

RF-EMF exposure might affect autophagy, namely degradation of damaged and aggregated proteins and may therefore trigger the development of neurodegenerative disorders. Autophagy markers ATG5 and LC3B-I and II and pERK were studied in RF-EMF and sham-exposed cells. In this study, RF-EMF induced a slight increase in ATG5 by trend in SH-SY5Y cells after 2 h of exposure and ATG5 protein levels were significantly increased after 24 h when compared to the respective sham control. LC3B-I and II were only analysed in SH-SY5Y cells but not in N9 cells due to unspecific binding in the latter cells. In SH-SY5Y cells exposed to RF-EMF for 2 h, LC3B-I protein levels increased by trend and a tendency towards a downregulation of LC3B-II was found after 24 h of RF-EMF exposure, whereas pERK I and II remained unchanged. Not many studies on RF-EMF exposure and autophagy are available in the literature. Previously published data showed increased levels of genes related to autophagy and autophagosomes in the hippocampus but not in the brain stem in C57BL/6 mice after RF-EMF exposure at 835 MHz at 4 W/kg for 12 weeks (Kim et al., 2018). The more complex system, namely *in vivo* exposure of mice and analyses in two brain regions including neurons, microglia and other cell types cannot be directly compared to our findings in neuroblastoma and/or microglial cells.

Oxidative stress was investigated in RF-EMF and sham-exposed cells by measurements of GSH and H_2O_2. As expected, menadione treatment resulted in an increase in GSH levels, whereas RF-EMF exposure did not affect GSH levels in microglial cells. In SH-SY5Y cells, but not in N9 cells, RF-EMF exposure significantly decreased GSH after 6 h but no difference was found after 24 h of RF-EMF exposure, indicating a transient increase in oxidative stress. Similar findings have been reported in mice exposed to 2100 MHz RF-EMF. A 10 day RF-EMF exposure led to an increased oxidative stress and DNA damage but the effects was not apparent anymore after 40 days of exposure (Sahin et al., 2016). In addition, RF-EMF exposure for 60 days at 0.59 and 0.66 mW/kg led to an increase in oxidative stress markers and diminished GSH and SOD in male Fischer 344 rats (Megha et al., 2015). In contrast, oxidative stress and DNA damage was not altered in C57BL/6 mice after GSM RF-EMF exposure at 5 W/kg for 8 months (Jeong et al., 2018). In neurodegenerative diseases, formation of ROS and antioxidant defense have been reported to be unbalanced (Radi et al., 2014). Therefore, results obtained in this study might indicate that RF-EMF exposure could lead to an imbalance, but given the antioxidant defense is not compromised due to other stressors, the cells can handle the ROS increase. Neuronal cells have been demonstrated to undergo various metabolic changes during neuronal differentiation that are accompanied by ROS production (Agostini et al., 2016; Zheng et al., 2016; Almeida and Vieira, 2017), and there is evidence that RF-EMF impairs neuronal differentiation (Eghlidospour et al., 2017). Besides neuronal differentiation, oxidative stress has been related to the etiology and/or pathogenesis of neurodegenerative diseases and (Dias et al., 2013; Lugrin et al., 2014; Cacabelos, 2017; Islam, 2017; Sison et al., 2018). There is also evidence from *in vivo* studies that long-time RF-EMF exposure does not induce oxidative stress. Long-term RF-EMF exposure (1950 MHz, 5 W/kg) in C57BL/6 mice for 8 months for 2 h/day and 5 days/week did not induce oxidative stress and DNA damage, and no changes were found for apoptosis markers, astrocyte or microglia neuroinflammation markers in aging brains (Jeong et al., 2018). In aging brains, persistent oxidative stress and deficient radical scavenging abilities were related to impair of cognitive functions (Huang et al., 2015). On the other hand, preconditioning, namely a small increase in oxidative stress, was shown to stimulate the cell's adaptive response to oxidative stress, and could be considered neuroprotective (Akki et al., 2018).

In the present study, H_2O_2 levels were elevated after 24 h when compared to 2 h, but no differences between RF-EMF-exposed cells was found in both cell types. Furthermore, RF-EMF exposure for 2 h significantly reduced cytochrome c levels in N9 cells and this effect was not apparent anymore after RF-EMF exposure for 24 h. Increased NADH oxidation was found in HeLa cells after RF-EMF exposure at 0.24 mW/cm^2 for 5 and 10 min, indicating ROS production. ROS was reported to acvtivate MMPs to cleave and release Hb-EGF that binds to epidermal growth factor to activate the ERK cascade (Friedman et al., 2007). In addition to our findings, there is also evidence from *in vitro* studies demonstrating increased ROS levels in neuroblastoma cells after short-time exposure to GSM RF-EMF at SAR levels ranging from 0.21–6 W/kg (Marjanovic Cermak et al., 2018; Stefi et al., 2019). In contrast, ROS levels remained unchanged after RF-EMF exposure at SAR levels of 2 (Kang et al., 2014) and 5 W/kg (Luukkonen et al., 2009) alone or in combination of H_2O_2 in neuronal cell lines and in rat primary cortical neurons exposed to 1800 MHz at 2 W/kg (Xu et al., 2010). Supporting our data, several *in vivo* studies showed increased ROS generation in the brain after GSM RF-EMF exposure (Megha et al., 2015; Stefi et al., 2019) with oxidative stress increase, especially in the hippocampus of the animals at average SAR levels of 1.6–6 W/kg (Bouji et al., 2020; Singh et al., 2020). As a consequence of increased oxidative stress, 2.45 GHz RF-EMF exposure was found to lead to impaired learning and memory and expression of anxiety behaviour in rats (Varghese et al., 2018).

The MAPK ERK has been shown to be related to autophagy (Martinez-Lopez et al., 2013) and neuronal differentiation and neurodegeneration (Dagda et al., 2008; Qiao et al., 2012; Zheng et al., 2016). Activation of ERK, namely phosphorylation (pERK), was demonstrated after GSM RF-EMF exposure at very low SAR levels (0.07 mW/cm^2), whereas stress-related MAPKs such as JNK and p38 were not altered (Friedman et al., 2007). In contrast, pERK was not altered in the present study regardless of the time or cell type used. Besides the difference in the SAR level used, the exposure time, fibroblasts (Rat1) and cervical cancer cells (HeLa) were used in the study by Friedman et al., whereas SH-SY5Y and microglial cells were used in the present study. Interestingly, the ERK activation was transient and was only apparent after 5 and 15 min of RF-EMF exposure but returned to baseline levels after 30 min of exposure (Friedman et al., 2007). Hence, possible ERK activation might have been missed in the present study due to the longer exposure times used. RF-EMF exposure of SH-SY5Y cells for 24 h at 900 MHz and 0.35 W/kg resulted in an increase in ERK1/2 (Buttiglione et al., 2007). However, the RF-EMF exposure system differs from the one used in the present study as described above, and the SAR was substantially smaller. Previously published data from our group showed that GSM RF-EMF exposure at 4 W/kg for 24 h did not alter ERK1 and pERK1/2 and mitochondrial respiration was only impaired in SH-SY5Y cells under glucose deprivation (von Niederhausern et al., 2019). Corroborating our findings, increased phosphorylation of MAPK was not found in astrocytes after RF-EMF exposure (1763 MHz) at SAR levels of 2 and 20 W/kg for 30 and 60 min with and without addition of the tumor promotor 12-O-tetradecanoylphorbol 13-acetate (TPA) (Lee et al., 2006). Therefore, effects might have been missed in this study due to the times of exposure chosen. However, pERK was reported to peak in the sensory and supporting cells of the cochlea three to six hours after exposure to 120 dB noise for 2 h (Maeda et al., 2013).

5. Conclusions

The data do not give evidence for RF-EMF (935 MHz, 4 W/kg) causing apoptosis in SH-SY5Y and microglial cells. The time-dependent increase in the autophagy marker, ATG5 and the antioxidant, GSH was dependent on the cell type and the time of RF-EMF exposure with neuroblastoma cells being more susceptible than microglial cells. The transient increase in GSH indicates that GSM RF-EMF at SAR values above the standards might cause oxidative stress. Studies on underlying mechanisms explaining the transient effects of short-time RF-EMF exposure need to be performed.

Declaration of Competing Interest

All authors disclose any financial and personal relationships with other people or organizations that could inappropriately influence this work.

Acknowledgments

The authors thank Nadja Peduto for helping with the cell culture work and the radiation system maintenance. This study was funded by the Swiss Research Foundation for Electricity and Mobile Communication, Swiss Federal Institute of Technology (ETH).

References

Agostini, M., Romeo, F., Inoue, S., Niklison-Chirou, M.V., Elia, A.J., Dinsdale, D., Morone, N., Knight, R.A., Mak, T.W., Melino, G., 2016. Metabolic reprogramming during neuronal differentiation. Cell Death Differ. 23, 1502–1514.

Akki, R., Siracusa, R., Morabito, R., Remigante, A., Campolo, M., Errami, M., La Spada, G., Cuzzocrea, S., Marino, A., 2018. Neuronal-like differentiated SH-SY5Y cells adaptation to a mild and transient H_2O_2 -induced oxidative stress. Cell Biochem. Funct. 36, 56–64.

Almeida, A.S., Vieira, H.L.A., 2017. Role of cell metabolism and mitochondrial function during adult neurogenesis. Neurochem. Res. 42, 1787–1794.

Baan, R., Grosse, Y., Lauby-Secretan, B., El Ghissassi, F., Bouvard, V., Benbrahim-Tallaa, L., Guha, N., Islami, F., Galichet, L., Straif, K., 2011. Carcinogenicity of radiofrequency electromagnetic fields. Lancet Oncol. 12, 624–626.

Bouji, M., Lecomte, A., Gamez, C., Blazy, K., Villegier, A.S., 2020. Impact of cerebral radiofrequency exposures on oxidative stress and corticosterone in a rat model of Alzheimer's disease. J. Alzheimers Dis. 73, 467–476.

Buttiglione, M., Roca, L., Montemurno, E., Vitiello, F., Capozzi, V., Cibelli, G., 2007. Radiofrequency radiation (900 MHz) induces Egr-1 gene expression and affects cell-cycle control in human neuroblastoma cells. J. Cell. Physiol. 213, 759–767.

Cacabelos, R., 2017. Parkinson's disease: from pathogenesis to pharmacogenomics. Int. J. Mol. Sci. 18.

Chen, C., Ma, Q., Liu, C., Deng, P., Zhu, G., Zhang, L., He, M., Lu, Y., Duan, W., Pei, L., Li, M., Yu, Z., Zhou, Z., 2014. Exposure to 1800 MHz radiofrequency radiation impairs neurite outgrowth of embryonic neural stem cells. Sci. Rep. 4, 5103.

Chu, C.T., 2019. Mechanisms of selective autophagy and mitophagy: implications for neurodegenerative diseases. Neurobiol. Dis. 122, 23–34.

Consales, C., Merla, C., Marino, C., Benassi, B., 2012. Electromagnetic fields, oxidative stress, and neurodegeneration. Int. J. Cell Biol. 2012, 683897.

Dagda, R.K., Zhu, J.H., Kulich, S.M., Chu, C.T., 2008. Mitochondrially localized ERK2 regulates mitophagy and autophagic cell stress. Autophagy 4, 770–782.

Dias, V., Junn, E., Mouradian, M.M., 2013. The role of oxidative stress in Parkinson's disease. J. Parkinsons Dis. 3, 461–491.

Eghlidospour, M., Ghanbari, A., Mortazavi, S.M.J., Azari, H., 2017. Effects of radiofrequency exposure emitted from a GSM mobile phone on proliferation, differentiation, and apoptosis of neural stem cells. Anat. Cell Biol. 50, 115–123.

Ertilav, K., Uslusoy, F., Ataizi, S., Naziroglu, M., 2018. Long term exposure to cell phone frequencies (900 and 1800 MHz) induces apoptosis, mitochondrial oxidative stress and TRPV1 channel activation in the hippocampus and dorsal root ganglion of rats. Metab. Brain Dis. 33, 753–763.

Friedman, J., Kraus, S., Hauptman, Y., Schiff, Y., Seger, R., 2007. Mechanism of short-term ERK activation by electromagnetic fields at mobile phone frequencies. Biochem. J. 405, 559–568.

Guo, F., Liu, X., Cai, H., Le, W., 2018. Autophagy in neurodegenerative diseases: pathogenesis and therapy. Brain Pathol. 28, 3–13.

Hoyto, A., Luukkonen, J., Juutilainen, J., Naarala, J., 2008. Proliferation, oxidative stress and cell death in cells exposed to 872 MHz radiofrequency radiation and oxidants. Radiat. Res. 170, 235–243.

Huang, T.T., Leu, D., Zou, Y., 2015. Oxidative stress and redox regulation on hippocampal-dependent cognitive functions. Arch. Biochem. Biophys. 576, 2–7.

IARC Working Group on the Evaluation of Carcinogenic Risks to Humans, 2013. Non-ionizing radiation, part 2: radiofrequency electromagnetic fields. IARC Monogr. Eval. Carcinog. Risks Hum. 102, 1–460.

Islam, M.T., 2017. Oxidative stress and mitochondrial dysfunction-linked neurodegenerative disorders. Neurol. Res. 39, 73–82.

Jeong, Y.J., Son, Y., Han, N.K., Choi, H.D., Pack, J.K., Kim, N., Lee, Y.S., Lee, H.J., 2018. Impact of long-term RF-EMF on oxidative stress and neuroinflammation in aging brains of C57BL/6 mice. Int. J. Mol. Sci. 19.

Joubert, V., Leveque, P., Cueille, M., Bourthoumieu, S., Yardin, C., 2007. No apoptosis is induced in rat cortical neurons exposed to GSM phone fields. Bioelectromagnetics 28, 115–121.

Kang, K.A., Lee, H.C., Lee, J.J., Hong, M.N., Park, M.J., Lee, Y.S., Choi, H.D., Kim, N., Ko, Y.G., Lee, J.S., 2014. Effects of combined radiofrequency radiation exposure on levels of reactive oxygen species in neuronal cells. J. Radiat. Res. 55, 265–276.

Kim, J.H., Yu, D.H., Kim, H.J., Huh, Y.H., Cho, S.W., Lee, J.K., Kim, H.G., Kim, H.R., 2018. Exposure to 835 MHz radiofrequency electromagnetic field induces autophagy in hippocampus but not in brain stem of mice. Toxicol. Ind. Health 34, 23–35.

Kumar, A., Dhawan, A., Kadam, A., Shinde, A., 2018. Autophagy and mitochondria: targets in neurodegenerative disorders. CNS Neurol. Disord. Drug Targets 17, 696–705.

Kuster, N., Schonborn, F., 2000. Recommended minimal requirements and development guidelines for exposure setups of bio-experiments addressing the health risk concern of wireless communications. Bioelectromagnetics 21, 508–514.

Lee, J.S., Huang, T.Q., Kim, T.H., Kim, J.Y., Kim, H.J., Pack, J.K., Seo, J.S., 2006. Radiofrequency radiation does not induce stress response in human T-lymphocytes and rat primary astrocytes. Bioelectromagnetics 27, 578–588.

Lu, Y., He, M., Zhang, Y., Xu, S., Zhang, L., He, Y., Chen, C., Liu, C., Pi, H., Yu, Z., Zhou, Z., 2014. Differential pro-inflammatory responses of astrocytes and microglia involve STAT3 activation in response to 1800 MHz radiofrequency fields. PLoS One 9, e108318.

Lugrin, J., Rosenblatt-Velin, N., Parapanov, R., Liaudet, L., 2014. The role of oxidative stress during inflammatory processes. Biol. Chem. 395, 203–230.

Luukkonen, J., Hakulinen, P., Maki-Paakkanen, J., Juutilainen, J., Naarala, J., 2009. Enhancement of chemically induced reactive oxygen species production and DNA damage in human SH-SY5Y neuroblastoma cells by 872 MHz radiofrequency radiation. Mutat. Res. 662, 54–58.

Maeda, Y., Fukushima, K., Omichi, R., Kariya, S., Nishizaki, K., 2013. Time courses of changes in phospho- and total- MAP kinases in the cochlea after intense noise exposure. PLoS One 8, e58775.

Marjanovic Cermak, A.M., Pavicic, I., Trosic, I., 2018. Oxidative stress response in SH-SY5Y cells exposed to short-term 1800 MHz radiofrequency radiation. J. Environ. Sci. Health A Tox. Hazard. Subst. Environ. Eng. 53, 132–138.

Martinez-Lopez, N., Athonvarangkul, D., Mishall, P., Sahu, S., Singh, R., 2013. Autophagy proteins regulate ERK phosphorylation. Nat. Commun. 4, 2799.

Megha, K., Deshmukh, P.S., Banerjee, B.D., Tripathi, A.K., Ahmed, R., Abegaonkar, M.P., 2015. Low intensity microwave radiation induced oxidative stress, inflammatory response and DNA damage in rat brain. Neurotoxicology 51, 158–165.

Menzies, F.M., Fleming, A., Rubinsztein, D.C., 2015. Compromised autophagy and neurodegenerative diseases. Nat. Rev. Neurosci. 16, 345–357.

Mhatre, M., Floyd, R.A., Hensley, K., 2004. Oxidative stress and neuroinflammation in Alzheimer's disease and amyotrophic lateral sclerosis: common links and potential therapeutic targets. J. Alzheimers Dis. 6, 147–157.

Motawi, T.K., Darwish, H.A., Moustafa, Y.M., Labib, M.M., 2014. Biochemical modifications and neuronal damage in brain of young and adult rats after long-term exposure to mobile phone radiations. Cell Biochem. Biophys. 70, 845–855.

Neubauer, G., Feychting, M., Hamnerius, Y., Kheifets, L., Kuster, N., Ruiz, I., Schuz, J., Uberbacher, R., Wiart, J., Roosli, M., 2007. Feasibility of future epidemiological studies on possible health effects of mobile phone base stations. Bioelectromagnetics 28, 224–230.

Nikolova, T., Czyz, J., Rolletschek, A., Blyszczuk, P., Fuchs, J., Jovtchev, G., Schuderer, J., Kuster, N., Wobus, A.M., 2005. Electromagnetic fields affect transcript levels of apoptosis-related genes in embryonic stem cell-derived neural progenitor cells. FASEB J. 19, 1686–1688.

Qiao, J., Paul, P., Lee, S., Qiao, L., Josifi, E., Tiao, J.R., Chung, D.H., 2012. PI3K/AKT and ERK regulate retinoic acid-induced neuroblastoma cellular differentiation. Biochem. Biophys. Res. Commun. 424, 421–426.

Radi, E., Formichi, P., Battisti, C., Federico, A., 2014. Apoptosis and oxidative stress in neurodegenerative diseases. J. Alzheimers Dis. 42, S125–S152.

Roosli, M., Frei, P., Mohler, E., Hug, K., 2010. Systematic review on the health effects of exposure to radiofrequency electromagnetic fields from mobile phone base stations. Bull. World Health Organ. 88, 887–896F.

Sahin, D., Ozgur, E., Guler, G., Tomruk, A., Unlu, I., Sepici-Dincel, A., Seyhan, N., 2016. The 2100MHz radiofrequency radiation of a 3G-mobile phone and the DNA oxidative damage in brain. J. Chem. Neuroanat. 75, 94–98.

Schneider L., Giordano S., Zelickson B.R., Johnson M.S., Benavides G.A., Ouyang X., Fineberg N., Darley-Usmar V.M., Zhang J., 2011. Differentiation of SH-SY5Y cells to a neuronal phenotype changes cellular bioenergetics and the response to oxidative stress. Free Radic. Biol. Med. 51, 2007–2017.

Schuderer, J., Oesch, W., Felber, N., Spat, D., Kuster, N., 2004a. In vitro exposure apparatus for ELF magnetic fields. Bioelectromagnetics 25, 582–591.

Schuderer, J., Spat, D., Samaras, T., Oesch, W., Kuster, N., 2004b. In vitro exposure systems for RF exposures at 900 MHz. IEEE Trans. Microwave Theory Tech. 52, 2067–2075.

Singh, K.V., Gautam, R., Meena, R., Nirala, J.P., Jha, S.K., Rajamani, P., 2020. Effect of mobile phone radiation on oxidative stress, inflammatory response, and contextual fear memory in Wistar rat. Environ. Sci. Pollut. Res. Int. 27, 19340–19351.

Sison, S.L., Vermilyea, S.C., Emborg, M.E., Ebert, A.D., 2018. Using patient-derived induced pluripotent stem cells to identify Parkinson's disease-relevant phenotypes.

Curr. Neurol. Neurosci. Rep. 18.
Stefi, A.L., Margaritis, L.H., Skouroliakou, A.S., Vassilacopoulou, D., 2019. Mobile phone electromagnetic radiation affects amyloid precursor protein and alpha-synuclein metabolism in SH-SY5Y cells. Pathophysiology 26, 203–212.
Varghese, R., Majumdar, A., Kumar, G., Shukla, A., 2018. Rats exposed to 2.45GHz of non-ionizing radiation exhibit behavioral changes with increased brain expression of apoptotic caspase 3. Pathophysiology 25, 19–30.
von Niederhausern, N., Ducray, A., Zielinski, J., Murbach, M., Mevissen, M., 2019. Effects of radiofrequency electromagnetic field exposure on neuronal differentiation and mitochondrial function in SH-SY5Y cells. Toxicol. in Vitro 61, 104609.
Wang, H., Zhang, X., 2017. Magnetic fields and reactive oxygen species. Int. J. Mol. Sci. 18.
Xu, S., Zhou, Z., Zhang, L., Yu, Z., Zhang, W., Wang, Y., Wang, X., Li, M., Chen, Y., Chen, C., He, M., Zhang, G., Zhong, M., 2010. Exposure to 1800 MHz radiofrequency radiation induces oxidative damage to mitochondrial DNA in primary cultured neurons. Brain Res. 1311, 189–196.
Zhao, T.Y., Zou, S.P., Knapp, P.E., 2007. Exposure to cell phone radiation up-regulates apoptosis genes in primary cultures of neurons and astrocytes. Neurosci. Lett. 412, 34–38.
Zheng, X., Boyer, L., Jin, M., Mertens, J., Kim, Y., Ma, L., Ma, L., Hamm, M., Gage, F.H., Hunter, T., 2016. Metabolic reprogramming during neuronal differentiation from aerobic glycolysis to neuronal oxidative phosphorylation. Elife 5.
Zielinski, J., Moller, A.M., Frenz, M., Mevissen, M., 2016. Evaluation of endocytosis of silica particles used in biodegradable implants in the brain. Nanomed. Nanotechnol. Biol. Med. 12, 1603–1613.